

A Silicon Photonics Mach-Zehnder Interferometer

edX username: murdoc11

I. INTRODUCTION

To be completed later. Silicon photonics is a rapidly growing industry that has already seen large-scale commercialization in the telecommunications industry. Emerging and promising applications include biomedical sensing and quantum information processing. This class aims to teach the fundamentals of the design, fabrication, and testing of silicon photonic devices. The class takes a rapid approach intended to quickly introduce the student to the entire process including design, simulations, layout, layout review, fabrication, and automated testing and data analysis. In order to proceed quickly but still give meaningful hands-on experience, the class centers around a simple silicon photonic device: the Mach-Zehnder interferometer.

In a Mach-Zender interferometer, light is split and travels down two paths and then is recombined. If the two waveguides are not exactly identical in their lengths L or propagation constants β then the light will be in or out of phase when it is recombined. If the light from the two paths is in-phase there will be constructive interference and the light intensity in the combined path will be the same as that in the initial path. If the light is perfectly out of phase when recombined, destructive interference will occur. In a silicon photonic waveguide, the result destructive interference that the light couples into higher-order, dispersive waveguide modes and is lost so that the output waveguide has no light. The output of the interferometer is typically measured over a wavelength sweep so that oscillations are clearly visible between wavelengths that result in in-phase and out of phase recombination. The period of the oscillations is known as the free spectral range (FSR) and is a key parameter for characterizing the interferometer.

In this report, two waveguide parameters are varied in order to create a mismatch between the two waveguide arms of the interferometer, namely (1) the lengths and (2) the widths of the two waveguides. Varying the lengths creates a path-length mismatch ΔL , while varying the widths creates a mismatch in the propagation constant β because the waveguide width changes the effective index. These effects and their relationship to the FSR are described in Sec. II.

The interferometer FSR is directly connected to the group index n_g of the waveguide. In the analysis of experimental data in Sec. VI, n_g will be determined based on the measurements and compared with simulation results presented in Sec. III. This will provide insight into the effects of manufacturing variability and the accuracy of simulations. These are important things to take into consideration in the development of all silicon photonic devices.

II. THEORY

This section begins with a description of a compact polynomial model for a waveguide index of refraction. It then details the mathematical form of an interferometer transfer function and free spectral range, including the dependence of the FSR on group index n_g . The equations for the FSR are initially taken from the book "Silicon Photonics Design" by Chrostowski and Hochberg [1] which only describes interferometer path mismatch based on differences in waveguide length. Because this report will also explore interferometers where the two paths have identical lengths but different widths, a more detailed derivation is presented for the FSR of this type of interferometer. Following this derivation, tables are given which outline the parameter variations and predicted FSR for all devices which will be tested.

A. Compact waveguide model

The properties of a waveguide can be described using a compact polynomial model for the index of refraction, as described in [1]. The index of refraction n is Taylor expanded as a function of wavelength λ (μm) as

$$n(\lambda) = n_1 + n_2(\lambda - \lambda_0) + n_3(\lambda - \lambda_0)^2. \quad (1)$$

The parameters n_1 (unit-less), n_2 (μm^{-1}), and n_3 (μm^{-2}) can be obtained through polynomial fitting (such as a least-squares fit method) once $n(\lambda)$ is calculated through a finite-difference eigenmode (FDE) or similar simulation of a waveguide.

As described in [1], these parameters can also be converted to the more traditional parameters

$$\begin{aligned} n_{\text{eff}} &= n_1 \\ n_g &= n_1 - n_2 \cdot \lambda_0 \\ D &= -2 \cdot \lambda_0 \cdot n_3/c \end{aligned} \quad (2)$$

where n_{eff} is the waveguide effective index, n_g is the group index, and D is the waveguide dispersion.

B. Interferometer transfer function and free spectral range

The transfer function for a simple Mach-Zehnder interferometer is given by equation (4.19c) in [1] as

$$\frac{I_o}{I_i} = \frac{1}{2} [1 + \cos(\beta_1 L_1 - \beta_2 L_2)] \quad (3)$$

$$\beta = \frac{2\pi n(\lambda)}{\lambda} \quad (4)$$

Here β_1 and β_2 are the wavenumbers of the two waveguides and L_1 and L_2 are the lengths of the waveguides. This equation neglects overall loss and applies to single-mode waveguides where only the total field intensity is considered in each waveguide.

If the imbalance in the two interferometer arms is created by a waveguide length mismatch $\Delta L = L_2 - L_1$, the free spectral range (FSR) of an interferometer (in meters) is given by equation (4.20b) in [1] as

$$\text{FSR} = \frac{\lambda_0^2}{n_g \Delta L} \quad (5)$$

where λ_0 is the wavelength around which the FSR is measured.

In Sec. VI the group index of the fabricated waveguides will be determined based on the FSR found in the experimental data. This is be easily obtained by solving Eq. (5) for n_g such that

$$n_g = \frac{\lambda^2}{\text{FSR} \cdot \Delta L}. \quad (6)$$

To extract n_g from the experimental data, the period of the interferometer fringes (the FSR) will be determined numerically around a chosen wavelength λ (e.g. 1550 nm). The measured FSR, the chosen λ , and the known ΔL from the layout will be substituted into Eq. (6) to determine the experimentally-measured waveguide group index.

C. Free spectral range for a waveguide-width-mismatched interferometer

To determine the FSR for devices which have a mismatch in waveguide width (so that $n_1 \neq n_2$), but no mismatch in the waveguide length ($L_1 = L_2$), we start with Eq. (3) The period (FSR) of the transfer function is determined by the phase

$$\delta = (\beta_1 - \beta_2)L.$$

The FSR is the wavelength difference between adjacent peaks $\Delta\lambda = \lambda_{m+1} - \lambda_m$. The phase difference between adjacent peaks is always 2π , or in other words,

$$\begin{aligned} 2\pi &= \delta_m - \delta_{m+1} \\ &= (\beta_{1,m} - \beta_{2,m})L - (\beta_{1,m+1} - \beta_{2,m+1})L. \end{aligned}$$

Rearranging and writing

$$\begin{aligned} \Delta\beta_1 &= \beta_{1,m} - \beta_{1,m+1} \\ \Delta\beta_2 &= \beta_{2,m} - \beta_{2,m+1} \end{aligned}$$

we have

$$\frac{2\pi}{L} = \Delta\beta_1 - \Delta\beta_2. \quad (7)$$

We can approximate that $\Delta\beta$ varies linearly with λ as

$$\Delta\beta = -\left.\frac{d\beta}{d\lambda}\right|_{\lambda_0} \Delta\lambda$$

and we can evaluate $\frac{d\beta}{d\lambda}$ at λ_0 since $\beta = \frac{2\pi n(\lambda)}{\lambda}$, which is

$$\left.\frac{d\beta}{d\lambda}\right|_{\lambda_0} = -\frac{2\pi}{\lambda_0^2} \left(n - \left.\frac{dn}{d\lambda}\right|_{\lambda_0} \lambda_0 \right) = -\frac{2\pi}{\lambda_0^2} n_g.$$

Plugging these into Eq. (7) we have an equation we can solve for $\Delta\lambda$ (the FSR):

$$\frac{2\pi}{L} = \frac{2\pi}{\lambda_0^2} (n_{1,g} - n_{2,g}) \Delta\lambda. \quad (8)$$

This results in

$$\text{FSR} = \Delta\lambda = \frac{\lambda_0^2}{L \Delta n_g}. \quad (9)$$

TABLE I
INTERFEROMETERS WITH LENGTH-MISMATCH

Device num	w	ΔL	n_{eff}	n_g	FSR
1	500 nm	100 μm	2.45	4.20	5.72 nm
2	500 nm	200 μm	2.45	4.20	2.86 nm
3	450 nm	100 μm	2.35	4.29	5.60 nm
4	550 nm	100 μm	2.52	4.12	5.83 nm
5	600 nm	100 μm	2.57	4.06	5.92 nm

TABLE II
INTERFEROMETERS WITH WIDTH-MISMATCH

Device num	w_1	w_2	L	FSR
6	500 nm	450 nm	900 μm	29.7 nm
7	500 nm	550 nm	900 μm	33.4 nm
8	500 nm	600 nm	900 μm	19.1 nm

D. Device parameter variations

In order to evaluate the effects of changing various parameters, the Mach-Zehnder interferometers will be designed, simulated, and fabricated across a sweep of waveguide *length* mismatches ΔL and a sweep of waveguide *width* mismatches. These parameters are shown in Tables I and II.

The devices in Table I have varying length mismatches between the two waveguides in the interferometer, but the widths of the two waveguides are identical. The FSR, n_{eff} , and n_g are evaluated at 1550 nm. The FSR is calculated using Eq. (5) while n_{eff} and n_g are taken from simulated data shown in Sec. III. The devices in Table II have varying width mismatches between the two waveguides, while the lengths of the two arms of the interferometer are identical. The FSR is evaluated at 1550 nm and is calculated using Eq. (9).

III. MODELING AND SIMULATION

Waveguides with widths 450 nm to 600 nm (as listed in Tables I and II) were simulated using Lumerical MODE™ software in order to obtain mode profiles and refractive indices. The simulation results presented here are for the TE mode.

Figs. 2 and 3 display the simulated values of n_{eff} and n_g as functions of wavelength from 1500 nm to 1600 nm. Note that while n_{eff} increases with increasing waveguide width, n_g decreases.

The values extracted from these simulations allow a compact model of the form of Eq. (1) to be written for these specific waveguides. The extracted values of n_1 , n_2 , and n_3 are listed in Table III.

Simulated mode profiles are shown in Fig. 1. The geometries of the waveguides are shown superimposed as white

TABLE III
WAVEGUIDE COMPACT MODEL PARAMETERS

Width	n_1	n_2 (μm^{-1})	n_3 (μm^{-2})
450 nm	2.353	-1.251	-0.037
500 nm	2.445	-1.131	-0.043
550 nm	2.513	-1.036	-0.027
600 nm	2.567	-0.962	-0.008

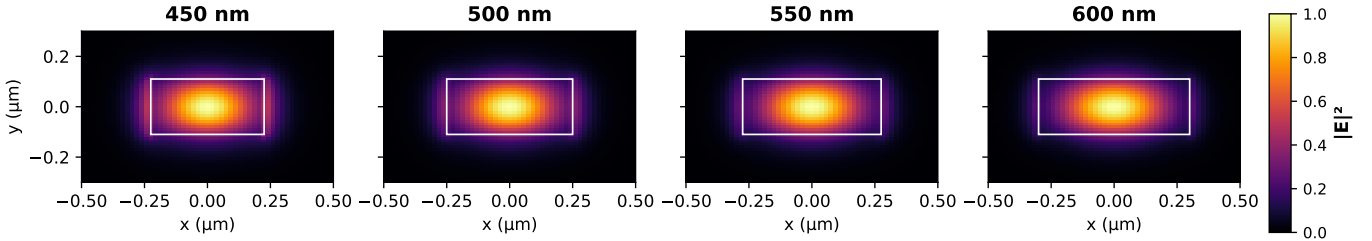


Fig. 1. Simulated mode profiles (electric field intensity $|E|^2$) at varying waveguide widths.

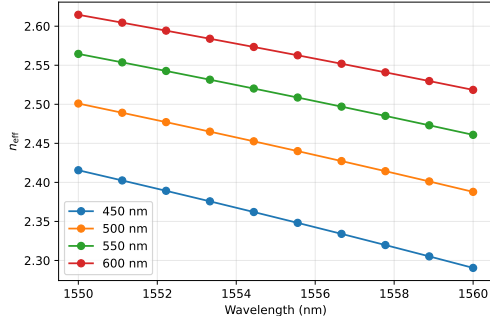


Fig. 2. Effective indices n_{eff} for waveguides of varying width.

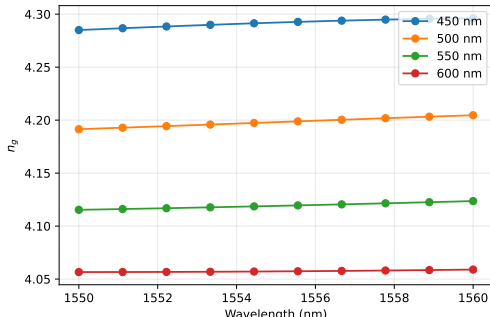


Fig. 3. Group indices n_g for waveguides of varying width.

rectangles. Notice that for the narrower waveguide (left-most), the mode profile leaks out the edges of the waveguide more so than it does for the widest waveguide (right-most). This size and strength of this evanescent wave is what determines the effective waveguide index and also has effects on the propagation loss of the waveguide.

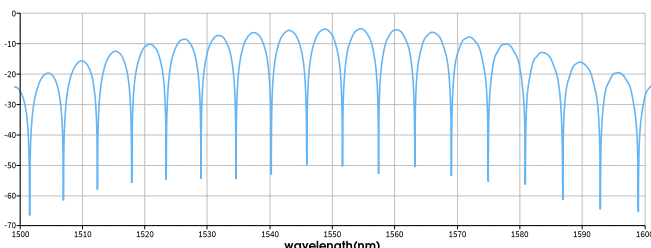


Fig. 4. Simulated transmission of device 1, a MZI with ΔL of $100 \mu\text{m}$ and waveguide width 500 nm .

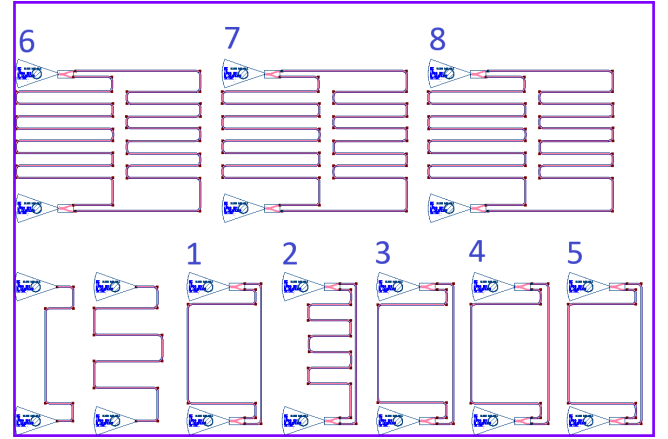


Fig. 5. Layout of the devices to be fabricated. Two de-embedding devices consisting of only a central MZI section.

The optical transfer function is simulated for device 2 (see Table I) using Lumerical INTERCONNECT™. The output is shown in Fig. 4. Clear dips are visible at wavelengths where total destructive interference is occurring. The overall shape of the spectrum including the fact that it never reaches a no-loss wavelength (which would correspond to 0 dB) are due to the wavelength dependent loss of the grating couplers used to get light on and off of the silicon photonic chip.

The FSR of the simulated spectrum is approximately 5.7 nm. This agrees well with the calculated value shown in Table I. This extracted FSR value can be used to calculate the group index n_g according to Eq. (6) which results in a value of 4.21. This agrees well with the value of 4.20 that can be calculated based on the parameters of Table III plugged into Eq. (2).

IV. FABRICATION

To be completed later (will include layout and details about fabrication).

See Fig. 5.

V. EXPERIMENTAL DATA

To be completed later.

VI. ANALYSIS

To be completed later.

VII. CONCLUSION

To be completed later.

REFERENCES

- [1] L. Chrostowski and M. Hochberg, *Silicon Photonics Design*, 1st ed. Cambridge University Press, 2015.